International Journal of Applied Science and Engineering

Special Issue-12th International Conference on Awareness Science and Technology (iCAST 2023)

Enhancing road marking sign detection in low-light conditions with YOLOv7 and contrast enhancement techniques

William Eric Manongga [1], Rung-Ching Chen [1*], Xiaoyi Jiang [2]

[1] *Department of Information Management, Chaoyang University of Technology, Taichung City 413310, Taiwan*
[2] *Faculty of Mathematics and Computer Science, University of Münster Schlosspl. 2, 48149 Münster, Germany*

ABSTRACT

Detecting road marking signs is a pivotal aspect of advanced driver-assisted systems (ADAS) and autonomous driving, providing crucial input for decision-making. However, the accuracy of road sign marking detection can be significantly affected by environmental factors, particularly in low-light conditions such as during night-time or within tunnels. In our research, we utilized two variants of YOLOv7, standard YOLOv7 and YOLOv7-tiny, combined with contrast enhancement techniques to enhance the detection of road marking signs, specifically focusing on low-light scenarios. Contrast-limited adaptive histogram equalization (CLAHE) and linear image fusion are employed and tested to detect road marking signs at night. The Taiwan road marking sign dataset at night (TRMSDN) is used in this research. Our evaluation results, comparing standard YOLOv7 and YOLOv7-tiny, revealed that leveraging contrast enhancement techniques can improve detection performance in low-light conditions. Our proposed method, which combines linearly fused images shows superior performance with 0.735 precision, 0.874 recall, 0.843 mAP@.5, and 0.798 F1-score for standard YOLOv7. YOLOv7-tiny achieves 0.782 precision, 0.843 recall, 0.850 mAP@.5, and 0.811 F1-score. Additionally, our experiment showcased that YOLOv7-tiny performs comparably to the standard YOLOv7 in detecting road marking signs, making it a viable option for deployment in edge devices. The limitation of the study is the usage of a constant weight during linear fusion and the limited number of images and classes in the dataset. Further research will try to address the limitation by investigating an adaptive weight value and increasing the number of data in the dataset.

Keywords: CLAHE, Contrast enhancement, Object detection, Road sign marking, YOLOv7.

OPEN ACCESS

Received: December 21, 2023
Revised: February 20, 2024
Accepted: March 19, 2024

Corresponding Author:
Rung-Ching Chen
crching@cyut.edu.tw

Publisher:
Chaoyang University of Technology
ISSN: 1727-2394 (Print)
ISSN: 1727-7841 (Online)

1. INTRODUCTION

The development of technology and economic expansion has led to a staggering rise in the global automobile population. As a part of people's daily life, cars shorten travel time and help people to travel more efficiently. However, with the increasing number of cars, the traffic system has become more complex, leading to a rise in traffic congestion and accidents. In recent years, intelligent transportation systems have come to help reduce or solve these problems by helping people to travel more efficiently and safely.

Globally, road traffic accidents are estimated to be the eighth leading cause of death. The World Health Organization (WHO) reports that 1.35 million people died because of car accidents in 2016, a number predicted to grow, potentially becoming the seventh

leading cause of death by 2030. The escalating death signals a pressing need for intervention to curtail these devastating outcomes.

The growth of AI and technology in the automotive industry plays a significant role in preventing fatal road accidents that lead to death and injuries. The advanced driver assistant systems (ADAS) and autonomous driving are key technologies aimed at increasing the safety while driving and reducing the number of road accidents. These technologies strive to revolutionize the driving experience by introducing proactive safety measures, pre-emptive accident avoidance mechanisms, and enhanced response capabilities, thereby creating a safer driving environment for all road users.

The detection and recognition of road marking signs play a pivotal role in the advancement of ADAS and autonomous driving. These signs provide crucial inputs for ADAS and during the decision-making of autonomous driving. In recent years, many strategies have been developed for detecting road marking signs (Greenhalgh and Mirmehdi, 2015; Lee et al., 2017; Gupta and Choudhary, 2018; Hoang et al., 2019; Tian et al., 2020). YOLO model has also been applied in various monitoring application (Chen et al., 2021). Presently, deep learning approaches are the most popular techniques to detect road marking signs due to their superior performance. However, the detection performance can be significantly affected by environmental factors. Low-light conditions, for instance, can reduce the accuracy and performance of road sign marking detection. To address the issue, we propose the combination of contrast enhancement techniques and YOLOv7 to improve the detection performance of road sign markings at night. Two contrast enhancement techniques, contrast limited adaptive histogram equalization (CLAHE) (Pizer et al., 1987) and linear image fusion, have been applied and tested. YOLOv7 (Wang et al., 2023), a state-of-the-art object detection method, has been chosen as the object detection algorithm for detecting road sign markings.

This paper is an extension paper from our previous conference paper published in iCAST2023 (Dewi et al., 2023). The main difference between the current research and the previous research lies on the version of YOLO model and the contrast enhancement techniques employed. The previous research employed YOLOv5, while the current research is using YOLOv7, which is a newer and better version of YOLO. We also used CLAHE and linear image fusion contrast enhancement technique, compared to contrast stretching which is used in the previous research.

The key contributions of our research are: (1) Analysing the effect of contrast enhancement techniques in improving the detection of road sign markings at night. (2) Analysing the benefits and drawbacks of using YOLOv7, specifically the standard YOLOv7 and YOLOv7-tiny, in detecting and recognizing Taiwan road marking signs at night.

The remaining sections of this paper are organized as follows. Section 2 provides the relevant works and our proposed methodology is described in section 3. Section 4 details the experiments and the results and section 5 presents the conclusion of our research.

2. RELATED WORKS

2.1 You Only Look Once (YOLOv7)

YOLOv7 (Wang et al., 2023) is a new addition to the YOLO family, representing a single-stage object detection method. It builds upon the advancements of YOLOv4 by incorporating the extended efficient long-range attention network (E-ELAN), introducing a new model scaling method for concatenation-based models, and employing a new reparameterization method to strike a balance between detection speed and accuracy.

Fig. 1 illustrates the network architecture of YOLOv7. The backbone comprises three blocks of convolution and batch normalization, followed by SILU activation function. This is succeeded by the E-ELAN and max pooling blocks, which performs down-sampling of the image into different scales. Within the neck, exists an SPPCSPC block– a CSPNet with an SPP block. Subsequently, a sequence of convolution up-sampling, and concatenation processes occurs before going through another E-ELAN block, down-sampling and finally reaching the head of the network. There are three network heads with RepConv (Ding et al., 2021) blocks that provide detections in various scales.

The capabilities of YOLOv7 is shown by research in many fields, including medical (Sun and Cong, 2022; Abdusalomov et al., 2023; Aşantoğrol and Çiftçi, 2023), agriculture (Wu et al., 2022; Cai et al., 2023), and road environment sensing (Kaya et al., 2023; Li et al., 2023; Tang et al., 2023).

2.2 Contrast Enhancement

Nowadays, obtaining digital images is incredibly easy. Digital cameras are a ubiquitous part of our daily lives and are available in various forms, from smartphones and security cameras to car dashboard cameras. However, one issue with digital images is the degradation of image quality due to low contrast. Thus, contrast enhancement techniques are sought to improve the visual quality of images. Low-contrast images generally exhibit a narrow histogram distribution. Contrast enhancement techniques effectively expand the distribution to enhance the contrast.

Numerous contrast enhancement techniques exist, with one of the simplest and most popular techniques being histogram equalization (HE) (Gonzales and Woods, 2018). HE modifies the pixel distribution using the cumulative distribution function. However, HE faces an over-enhancement problem, especially with images having varying local contrast. Adaptive histogram equalization was subsequently designed to address the over-enhancement issue. CLAHE (Pizer et al., 1987) stands out as one of the popular adaptive histogram equalization techniques.

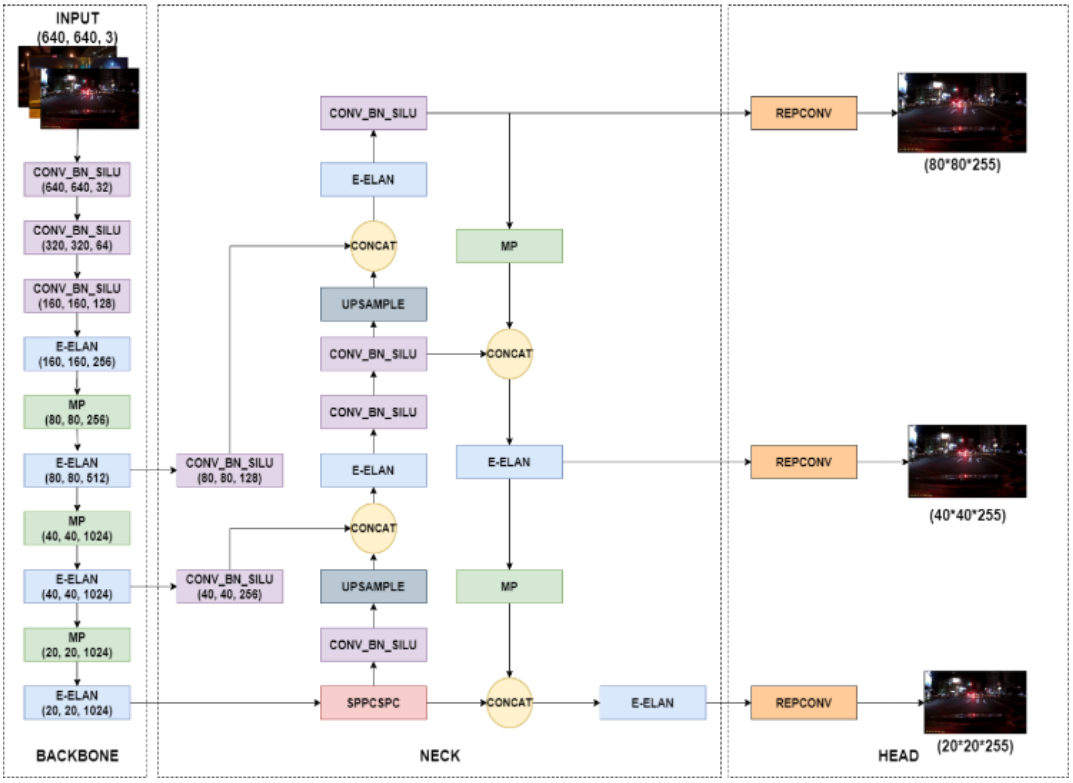

Fig. 1. Original YOLOv7 architecture

Another approach to appropriately enhance image contrast is by applying linear combination. Manongga et al. (2023) and Hsieh et al. (2010) showed in their research that a linear combination of two images can improve the image contrast while preventing over-enhancement.

In object detection, contrast enhancement has been widely used in research to improve the detection accuracy. In the medical field, Nneji et al. (2022) utilized CLAHE on CT images to enhance image contrast and features for pneumonia detection. To improve the detection of COVID-19, Benradi et al. (2022) employed HE on the radiology images. Contrast enhancement is also extensively used to improve cancer detection (Srinivasan et al., 2023) and tumor identification (Ramamoorthy et al., 2022). In agriculture, Babu and Ram (2022) utilized adaptive histogram equalization to enhance the weed detection in soybean crops. It can aid in the identification of plant leaf disease (Zamani et al., 2022). Moreover, contrast enhancement can be utilized in the manufacturing industry to enhance accuracy in detecting production defects (Sari and Ulas, 2022; Pathak and Patil, 2023).

2.3 Road Marking Sign Detection

Road marking sign detection is an essential part of intelligent transportation system. Both ADAS and autonomous vehicles rely on the detection of road marking sign and other traffic signs to make decision and inform or warn the driver if any dangerous situation occurs. To design a fast and accurate road marking sign detection is a popular research domain in computer vision.

A method of extracting road marking signs and matching them to the pattern was introduced by Foucher et al. (2011). Ding et al. (2015) use the combination of histogram of oriented gradient (HOG) and support vector machine (SVM) to recognize and categorize five categories of road marking signs. Newer research using deep learning was done by Dewi et al. (2022), which employs YOLOv5 to detect Taiwan road marking signs.

3. METHODOLOGY

3.1 Proposed Method

Fig. 2 illustrates the methodology adopted in our research. Our research can be divided into three main parts: image enhancement, model training, and model evaluation and result analysis. In the image enhancement part, we begin with the original TRMSDN dataset and apply two different image enhancement techniques to improve the image contrast. The first method utilized is CLAHE, while the second method utilized linear image combination.

The process of CLAHE comprised the following five steps:

1. Image division: divide the original image into smaller regions or tiles. The size and number of tiles may vary based on the desired level of local contrast enhancement. In our experiment, we choose the number of tiles to be 64 (8 × 8).
2. Histogram calculation: calculate the histogram of pixel intensity for each tile.
3. Histogram equalization: apply histogram equalization to each individual tile.

4. Contrast limiting: limit the amplification of intensities in each tile by clipping the contrast enhancement when the value exceeds a certain threshold.
5. Interpolation and assembly: combine all the processed tiles to reconstruct the entire enhanced image. Interpolation techniques are used to smoothen the transition between tiles.

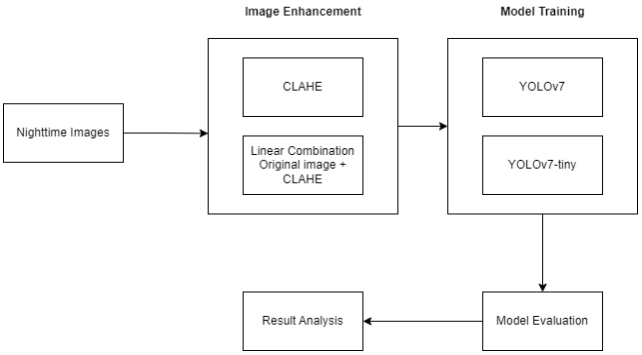

Fig. 2. Research flow

Linear image combination involved merging the original image from the dataset with the CLAHE-enhanced image. The final enhanced image is obtained by the Equation (1).

$$I_e = wI_{ori} + (1 - w)I_{CLAHE} \quad (1)$$

Where I_e is the final enhanced image; w represents the weight of the image; I_{ori} is the original image; and I_{CLAHE} denotes the CLAHE enhanced image. For our experiment, we set the value of w to 0.5, providing equal weight to the original image and CLAHE-enhanced image during the combination. The value of 0.5 is chosen because the optimum value w depends on the condition of the original image and the enhanced image. An optimum w value will balance the increase in brightness while still preserving the important features from both images. However, the calculation of the optimum value will take some considerable time and might cause the solution to not be able to work in real-time. Hence, the value of 0.5, which is the balance between the original image and CLAHE enhanced image while giving a proportionally enhanced image.

Fig. 3. Three sets of images obtained from the original dataset after contrast enhancement

Following the image enhancement process, we obtained three sets of images of from the dataset: the original image, the CLAHE-enhanced images and linearly-combined images. Fig. 3 displays an example of the images in the dataset.

The subsequent step involved training the YOLOv7 model using these three versions of the dataset. In our research, we opted for two versions of YOLOv7: the standard YOLOv7 and YOLOv7-tiny. YOLOv7-tiny is included in our research due to its capability to run on edge devices, a crucial requirement for numerous ADAS systems. All the models were trained for 100 epochs, utilizing an image dimension of 640 × 640 pixels and the batch size configured to 32. The trained model will then be evaluated and the result will be analyzed and compared to draw the final conclusion of the research.

3.2 Dataset

In our research, we focused our experiment on the general road signs available in Taiwan. We utilized the Taiwan road marking sign dataset at night (TRMSDN) (Chen et al., 2023) , comprising images with dimensions of 512 × 288 pixels. These images were captured using dashboard cameras during night-time driving in Taiwan and have varied and dynamic lighting conditions that depicts the natural night-time driving. The dataset encompasses 12 classes representing the common road marking signs in Taiwan, with each class containing approximately 400 images, totalling 4386 images in the dataset. The dataset is split into the training and testing in an 80 : 20 ratio. Detailed information about the dataset is provided in Table 1.

3.3 Evaluation Metrics

To evaluate the proposed method, precision, recall, and mAP (mean average precision) are utilized as evaluation metrics. Precision represents the proportion of positive predictions while accounting for false positives. In simple terms, it determines the accuracy of positive predictions among all the predicted positive instances. The formula for precision is expressed by Equation (2).

$$Precision = \frac{TP}{TP+FP} \quad (2)$$

Recall, on the other hand, signifies the ratio of positive predictions while considering false negatives. It evaluates how many of the actual positive cases were predicted as positive. The calculation for recall is given by Equation (3).

$$Recall = \frac{TP}{TP+FN} \quad (3)$$

Table 1. TRMSND details

Class	Name	Images
P1	Turn right	405
P2	Turn left	401
P3	Go straight	407
P4	Turn right or go straight	409
P5	Turn left or go straight	403
P6	Speed limit (60)	400
P7	Crosswalk	401
P8	Slow sign	399
P9	Overtaking prohibited	404
P10	Barrier line	409
P11	Cross hatch	398
P12	Stop line	403
Total		4386

True positives (TP) are the cases where the model correctly predicts the positive class. False positive (FP) occurs when the model incorrectly predicts the positive class. False negatives (FN) happen when the model fails to predict the positive class.

Additionally, mAP is computed by determining the average precision (AP) for each class. It accounts for the trade-off between precision and recall, making it a suitable metric for most detection applications. The formula of mAP is denoted by Equation (4).

$$mAP = \frac{1}{N}\sum_{i=1}^{N} AP_i \quad (4)$$

Where N is the number of classes; and AP_i is the AP for class i. In our research, we use mAP@.5, which is the mAP value with 50% IoU (intersection over union), which means that a detection is only considered as a correct detection if the IoU value is higher than 50%.

4. RESULTS AND DISCUSSION

In this section, we present the experimental result of night-time road ground sign detection at night using YOLOv7 and YOLOv7-tiny. Firstly, we will review the training and testing results of both YOLOv7 models. Following that, we will delve into discussing the performance disparity between standard YOLOv7 and YOLOv7-tiny, as well as the impact of image enhancement techniques on enhancing detection performance. We also compare our results with our previous research which was done using YOLOv5s and contrast stretching (Dewi et al., 2023).

4.1 Training Result

Table 2 displays the training result of standard YOLOv7 utilizing the original image, the CLAHE image, and the linear combined image. The results highlight that the model trained using the original image achieves superior precision. However, the model trained using CLAHE image obtained the best recall and mAP@.5. Interestingly, the model trained on the linear combined image does not yield the best scores in any of the three metrics. Nevertheless, it still outperforms the model trained on the original image in terms of both recall and mAP@.5.

Table 3 showcases the training result for YOLOv7-tiny. The model trained on the original image displays higher recall score, whereas the model trained on linear combined image attains the highest precision and mAP@.5 scores. Although the model utilizing the CLAHE image doesn't secure the top score in all three metrics, it achieves slightly lower scores on recall and mAP@.5.

Table 2. Training result of standard YOLOv7

Class	Images	Labels	Original image			CLAHE image			Linear combined image		
			P	R	mAP@.5	P	R	mAP@.5	P	R	mAP@.5
P1	3509	310	0.774	0.945	0.953	0.764	0.984	0.961	0.769	0.971	0.959
P2	3509	306	0.747	1.000	0.932	0.749	0.997	0.946	0.748	0.984	0.938
P3	3509	334	0.738	0.967	0.906	0.737	0.994	0.922	0.770	0.961	0.919
P4	3509	316	0.714	0.990	0.945	0.709	0.994	0.948	0.698	0.994	0.951
P5	3509	275	0.695	0.996	0.905	0.692	0.995	0.912	0.694	0.993	0.906
P6	3509	291	0.965	0.997	0.995	0.955	0.997	0.995	0.983	0.998	0.996
P7	3509	329	0.616	0.771	0.702	0.580	0.869	0.719	0.599	0.781	0.695
P8	3509	321	0.964	0.997	0.991	0.940	1.000	0.991	0.969	1.000	0.992
P9	3509	308	0.973	0.997	0.992	0.974	0.997	0.992	0.982	1.000	0.993
P10	3509	524	0.759	0.877	0.895	0.764	0.906	0.924	0.777	0.858	0.909
P11	3509	310	0.838	0.990	0.964	0.833	0.997	0.972	0.832	0.991	0.949
P12	3509	284	0.741	0.222	0.378	0.600	0.328	0.368	0.619	0.292	0.388
All	3509	3908	**0.794**	0.896	0.880	0.775	**0.921**	**0.887**	0.787	0.902	0.883

Table 3. Training result of YOLOv7-tiny

Class	Images	Labels	Original image			CLAHE image			Linear combined image		
			P	R	mAP@.5	P	R	mAP@.5	P	R	mAP@.5
P1	3509	310	0.743	0.977	0.953	0.756	0.971	0.952	0.885	0.881	0.955
P2	3509	306	0.744	0.984	0.943	0.741	0.987	0.922	0.895	0.928	0.941
P3	3509	334	0.719	0.982	0.908	0.720	0.979	0.897	0.917	0.96	0.914
P4	3509	316	0.696	0.991	0.946	0.722	0.984	0.949	0.886	0.929	0.951
P5	3509	275	0.690	0.993	0.910	0.687	0.993	0.914	0.893	0.942	0.926
P6	3509	291	0.956	0.997	0.993	0.952	0.997	0.995	0.991	0.993	0.995
P7	3509	329	0.583	0.830	0.699	0.593	0.805	0.695	0.793	0.772	0.681
P8	3509	321	0.924	1.000	0.991	0.948	1.000	0.993	0.949	0.993	0.991
P9	3509	308	0.978	0.997	0.990	0.974	0.990	0.993	0.974	0.997	0.991
P10	3509	524	0.721	0.851	0.869	0.725	0.868	0.883	0.711	0.823	0.861
P11	3509	310	0.826	0.984	0.952	0.825	0.977	0.943	0.956	0.987	0.952
P12	3509	284	0.595	0.294	0.337	0.657	0.249	0.354	0.267	0.276	0.354
All	3509	3908	0.765	**0.907**	0.874	0.775	0.900	0.874	**0.843**	0.873	**0.876**

4.2 Testing Results

After training the models, we proceed to evaluate the trained models on the test set. The evaluation results of YOLOv7 are presented in Table 4. The model trained on the original image achieved the highest precision, while the model trained on the linear combined image obtained the highest recall score and mAP@.5. Notably, the model trained on CLAHE images didn't secure the top score in any evaluation metrics, although the results were only marginally worse.

Table 5 presents the evaluation result for YOLOv7-tiny. Similar to the result of standard YOLOv7, the model trained on the linear combined image shows superior performance compared to the model trained on the original image and the CLAHE image, which is shown by the higher precision score and mAP@.5 value, while having a slightly lower recall score. The model trained using CLAHE image get the highest recall score. However, it also scored the lowest precision compared to other models.

Table 4. Testing result of standard YOLOv7

Class	Images	Labels	Original image			CLAHE image			Linear combined image		
			P	R	mAP@.5	P	R	mAP@.5	P	R	mAP@.5
P1	877	78	0.730	0.971	0.956	0.553	0.296	0.306	0.526	0.281	0.317
P2	877	76	0.694	0.934	0.873	0.752	0.949	0.950	0.735	0.949	0.949
P3	877	85	0.730	0.918	0.898	0.676	0.933	0.879	0.686	0.974	0.879
P4	877	80	0.689	0.887	0.891	0.702	0.918	0.888	0.738	0.941	0.894
P5	877	69	0.739	0.899	0.902	0.656	0.925	0.890	0.645	0.938	0.902
P6	877	73	0.960	0.982	0.994	0.681	0.927	0.878	0.672	0.928	0.891
P7	877	82	0.609	0.683	0.664	0.972	1.000	0.989	0.960	0.978	0.993
P8	877	78	0.925	0.962	0.983	0.592	0.805	0.684	0.571	0.829	0.702
P9	877	79	0.993	0.962	0.987	0.898	0.974	0.979	0.894	0.978	0.979
P10	877	128	0.569	0.742	0.713	0.975	0.980	0.995	0.982	0.987	0.986
P11	877	78	0.809	0.949	0.898	0.604	0.690	0.711	0.618	0.747	0.740
P12	877	71	0.525	0.296	0.342	0.812	0.962	0.922	0.791	0.962	0.881
All	877	977	**0.748**	0.849	0.842	0.739	0.863	0.839	0.735	**0.874**	**0.843**

Table 5. Testing result of YOLOv7-tiny

Class	Images	Labels	Original image			CLAHE image			Linear combined image		
			P	R	mAP@.5	P	R	mAP@.5	P	R	mAP@.5
P1	877	78	0.729	0.923	0.951	0.711	0.978	0.950	0.840	0.885	0.952
P2	877	76	0.678	0.908	0.887	0.649	0.961	0.868	0.753	0.895	0.884
P3	877	85	0.729	0.941	0.862	0.700	0.929	0.880	0.729	0.917	0.882
P4	877	80	0.642	0.912	0.873	0.650	0.912	0.883	0.732	0.886	0.904
P5	877	69	0.720	0.928	0.895	0.683	0.971	0.914	0.755	0.893	0.923
P6	877	73	0.960	0.996	0.995	0.949	1.000	0.995	0.948	0.991	0.995
P7	877	82	0.586	0.817	0.676	0.535	0.955	0.705	0.606	0.793	0.694
P8	877	78	0.893	0.987	0.988	0.882	0.974	0.976	0.935	0.949	0.981
P9	877	79	0.998	0.975	0.992	0.982	0.987	0.986	1	0.974	0.995
P10	877	128	0.645	0.727	0.704	0.537	0.781	0.726	0.642	0.711	0.75
P11	877	78	0.806	0.962	0.933	0.784	0.949	0.896	0.814	0.956	0.926
P12	877	71	0.585	0.238	0.284	0.470	0.268	0.317	0.633	0.267	0.319
All	877	977	0.748	0.859	0.837	0.711	**0.889**	0.841	**0.782**	0.843	**0.850**

4.3 Discussion

After reviewing the detection results in the previous section, there are some notable points to discuss. Firstly, we will compare the performance of YOLOv7 and YOLOv7-tiny in detecting road marking signs at night. Secondly, we will delve into how contrast enhancement techniques can enhance detection performance, especially in low-light conditions. Lastly, we will compare our results with our previous research and analyze them.

4.3.1 YOLOv7 vs YOLOv7-tiny

In our research, we conducted experiments with YOLOv7 and YOLOv7-tiny, the latter being specifically designed to run on edge devices. Our aim is to compare the number of parameters, inference speed, and the detection performance between the two models.

Table 6 displays the comparison between YOLOv7 and YOLOv7-tiny. The standard model, intended to run on normal GPUs, contains 37M parameters, whereas YOLOv7-tiny, is significantly smaller with only 6M parameters. The number of parameters also indicates the need of more computation power. The result highlights how YOLOv-tiny7 is far more lightweight compared to the standard model. When evaluated on Nvidia RTX4090 GPU, YOLOv7 processes an image in 7.5 ms (133 fps), while YOLOv7-tiny processes an image in 4.2 ms (238 fps). However, when run on CPU alone, both models require more time for inference. YOLOv7 takes 155.7 ms per image, equivalent to 6.4 fps. YOLOv7-tiny, which is designed for edge devices performs slightly better with 46 ms per image, approximately 21 fps. Notably, both versions exhibit high fps when run on a standard GPU, enabling real-time detection in practical scenarios. However, on a CPU, both models operate at slower speeds, and due to the absence of an edge GPU device, we were unable to test the models in such an environment.

Table 6. Comparison of YOLOv7 and YOLOv7-tiny

		YOLOv7	YOLOv7-tiny
Number of parameters		37.225.324	6.029.420
Inference speed	GPU (RTX 4090)	7.5 ms/image (133.33 fps)	4.2 ms/image (238 fps)
	CPU (Intel-Core i913900F)	155.7 ms/image (6.4 fps)	46 ms/image (21 fps)
Detection performance*	Precision	0.748	0.748
	Recall	0.849	0.859
	mAP@.5	0.842	0.837

*Evaluated on original images from TRMSND

In terms of detection performance, YOLOv7 exhibits lower precision compared to YOLOv7-tiny. However, YOLOv7 achieves higher recall and mAP@.5 scores. The difference in these scores, although noticeable, does not significantly impact the overall detection performance.

4.3.2 The impact of image enhancement on object detection performance

In this section, we delve into the impact of image enhancement techniques on improving detection performance. Table 7 presents the comparison of detection performance between YOLOv7 and YOLOv7-tiny using different sets of images. Since determining the superior method based on solely the precision and recall value can be challenging, we employ the F1-score, calculated by combining these two-evaluation metrics, to determine the best method.

For the standard YOLOv7 model, the model trained using the linear combined image achieves the highest F1-score of 0.798, followed by the model using CLAHE image. In contrast, the model trained on the original image scores the lowest among the three. On the other hand, the YOLOv7-tiny model using linear combined image also secures the best F1-score. However, the model using CLAHE images obtains the lowest score compared to the other models.

Linear image combination worked better than the original image and CLAHE enhanced image since it combines both images to produce a contrast enhanced image while still preserving the important features from the original image. This is very important, especially in real-world driving situations, given the varying ambient conditions.

Table 7. Detection performance using different set of images

Model	Image	P	R	mAP@.5	F1-score
YOLOv7	Original	**0.748**	0.849	0.842	0.795
	CLAHE	0.739	0.863	0.839	0.796
	Linear combined	0.735	**0.874**	**0.843**	**0.798**
YOLOv7-tiny	Original	0.748	0.859	0.837	0.799
	CLAHE	0.711	**0.889**	0.841	0.790
	Linear combined	**0.782**	0.843	**0.850**	**0.811**

The experiment results demonstrate that image enhancement techniques can enhance the performance of detection on YOLOv7. Although the F1-score of CLAHE image on the YOLOv7-tiny appears worse compared to the original image, the overall trend indicates improved performance across other experiments when utilizing image enhancement techniques.

4.3.3 Comparison with previous study

In this section, we compare our research results and our previous research. The previous study employed YOLOv5s, contrasting with our utilization of YOLOv7 and YOLOv7-tiny in the current research. Furthermore, the earlier study utilized a different contrast enhancement method, contrast stretching (CS), whereas in the current research, we employ CLAHE and linear combination.

Table 8 presents the performance comparison between the method in the previous study and our proposed approach. The results indicate that the previous method achieved a higher in term of recall score. However, our proposed method notably enhances the precision and mAP@.5. The method using standard YOLOv7 with linear combination improved the precision by 4.7%, while the using YOLOv7-tiny with linear combination enhanced the precision by 9.4%. In terms of mAP@.5, the use of YOLOv7 with linear combination improved the score by 0.5%, whereas YOLOv7-tiny with linear combination improved the score by 1.2%. The results of the experiments indicate that our proposed method exhibits better performance compared to the approach used in the previous research.

Table 8. Comparison with previous study

Method	Precision	Recall	mAP@.5
YOLOv5s + CS (Dewi et al., 2023)	68.8%	**89.5%**	83.8%
YOLOv7 + linear combination	73.5%	87.4%	84.3%
YOLOv7-tiny + linear combination	**78.2%**	84.3%	**85.0%**

5. CONCLUSION

In this experiment, we employed YOLOv7 and YOLOv7-tiny to detect road sign markings at night using both the original TRMSDN dataset and its enhanced version. Two image enhancement techniques are utilized in our experiment: CLAHE and linear combination of the original image and CLAHE image. Additionally, we compare the performance of the standard YOLOv7 and YOLOv7-tiny in detecting these road marking signs. The results indicate that YOLOv7-tiny demonstrates nearly comparable detection performance to standard YOLOv7. It can also run on edge devices which makes it a favorable choice when implementing computer vision systems.

The experiment using image enhancement techniques revealed that the model using the proposed linear combined image outperformed those using the original image and CLAHE enhanced images, for both YOLOv7 and YOLOv7-tiny, which highlights the effectiveness of image enhancement techniques improving the detection performance of road marking signs in night images. Comparison with our previous study also shows that our proposed method achieves superior performance, as shown by the higher precision and mAP@.5 score.

In the future, we will investigate the way to use adaptive weight on the linear image combination to provide a better image for the model to train and detect. We will also try to enhance the current dataset by adding more images to the dataset and also adding more classes to cover more types of road marking signs. The experiments of YOLOv7-tiny on edge device in a car is our future work.

ACKNOWLEDGMENT

This paper is supported by the National Science and Technology Council, Taiwan. The Nos are NSTC-112-2221-E-324-003-MY3 and NSTC-112-2221-E-324 -011.

REFERENCES

Abdusalomov, A.B., Mukhiddinov, M., Whangbo, T.K. 2023. Brain tumor detection based on deep learning approaches and magnetic resonance imaging. Cancers, 15(16), 4172.

Aşantoğrol, F., Çiftçi, B.T. 2023. Analytical comparison of maxillary sinus segmentation performance in panoramic radiographs utilizing various yolo versions. European Journal of Therapeutics, 29(4), 748–758.

Babu, V.S., Ram, N.V. 2022. Deep Residual CNN with Contrast limited adaptive histogram equalization for weed detection in soybean crops. Traitement Du Signal, 39(2), 717–722.

Benradi, H., Chater, A., Lasfar, A. 2022. Detection of COVID-19 from chest radiology using histogram equalization combined with a CNN convolutional network. ITM Web of Conferences, 46, 05001.

Cai, L., Liang, J., Xu, X., Duan, J., Yang, Z. 2023. Banana Pseudostem Visual detection method based on improved YOLOV7 detection algorithm. Agronomy, 13(4), 999.

Chen, R.-C., Dewi, C., Zhuang, Y.-C., Chen, J.-K. 2023. Contrast limited adaptive histogram equalization for recognizing road marking at night based on yolo models. IEEE Access, 11, 92926–92942.

Chen, R.-C., Saravanarajan, V. S., Hung, H.-T. 2021. Monitoring the behaviours of pet cat based on YOLO model and raspberry Pi. International Journal of Applied Science and Engineering, 18(5), 1–12.

Dewi, C., Chen, R.-C., Zhuang, Y.-C., Christanto, H. J. 2022. Yolov5 series algorithm for road marking sign identification. Big Data Cognitive Computing, 6(4),149.

Dewi, C., Chen, R.-C., Zhuang, Y.-C., Manongga, W. E. 2023. Contrast stretching for automatic road marking detection at night with YOLOv5. In 2023 12th International Conference on Awareness Science and Technology (iCAST), 100–105.

Ding, D., Yoo, J., Jung, J., Jin, S., Kwon, S. 2015. Efficient Road-sign detection based on machine learning. Bulletin of Networking, Computing, Systems, and Software, 4(1), 15–17.

Ding, X., Zhang, X., Ma, N., Han, J., Ding, G., Sun, J. 2021. RepVgg: Making VGG-style convnets great again. In Proceedings of the IEEE Computer Society Conference on Computer Vision and Pattern Recognition, 13728–13737.

Foucher, P., Sebsadji, Y., Tarel, J.-P., Charbonnier, P., Nicolle, P. 2011. Detection and recognition of urban road markings using images. In 2011 14th International IEEE Conference on Intelligent Transportation Systems (ITSC), 1747–1752.

Gonzales, R.C., Woods, R.E. 2018. Digital image processing, fourth edition. Pearson Education, Inc.

Greenhalgh, J., Mirmehdi, M. 2015. Detection and recognition of painted road surface markings. In ICPRAM 2015 - 4th International Conference on Pattern Recognition Applications and Methods, Proceedings (Vol. 1),130–138.

Gupta, A., Choudhary, A. 2018. A framework for camera-based real-time lane and road surface marking detection and recognition. IEEE Transactions on Intelligent Vehicles, 3(4), 476–485.

Hoang, T.M., Nam, S.H., Park, K.R. 2019. Enhanced detection and recognition of road markings based on adaptive region of interest and deep learning. IEEE Access, 7, 109817–109832.

Hsieh, C.H., Chen, B.C., Lin, C.M., Zhao, Q. 2010. Detail aware contrast enhancement with linear image fusion. In 2010 2nd International Symposium on Aware Computing, ISAC 2010 - Symposium Guide, 1–5.

Kaya, Ö., Çodur, M.Y., Mustafaraj, E. 2023. Automatic detection of pedestrian crosswalk with faster R-CNN and YOLOv7. Buildings, 13(4), 1070.

Lee, S., Kim, J., Yoon, J.S., Shin, S., Bailo, O., Kim, N., Kweon, I.S. 2017. VPGNet: Vanishing point guided network for lane and road marking detection and recognition. In Proceedings of the IEEE International Conference on Computer Vision, 1965–1973.

Li, S., Wang, S., Wang, P. 2023. A small object detection algorithm for traffic signs based on improved YOLOv7. Sensors, 23(16), 7145.

Manongga, W.E., Hsieh, C.H., Chen, R.C., Cheng, C.H. 2023. Optimal contrast enhancement with linear image fusion and patch-based contrast quality index. In 2023 International Conference on Consumer Electronics - Taiwan, ICCE-Taiwan 2023 - Proceedings, 787–788.

Nneji, G.U., Cai, J., Deng, J., Monday, H.N., James, E.C., Ukwuoma, C.C. 2022. Multi-channel based image processing scheme for pneumonia identification. Diagnostics, 12(2), 325.

Pathak, S.P., Patil, S.A. 2023. Evaluation of effect of pre-processing techniques in solar panel fault detection. IEEE Access, 11, 72848–72860.

Pizer, S.M., Amburn, E.P., Austin, J.D., Cromartie, R., Geselowitz, A., Greer, T., Zuiderveld, K. 1987. Adaptive histogram equalization and its variations. Computer Vision, Graphics, and Image Processing, 39(3), 355–368.

Ramamoorthy, M., Qamar, S., Manikandan, R., Jhanjhi, N.Z., Masud, M., Alzain, M.A. 2022. Earlier detection of brain tumor by pre-processing based on histogram equalization with neural network. Healthcare (Switzerland), 10(7), 1218.

Sari, F., Ulas, A.B. 2022. Deep learning application in detecting glass defects with color space conversion and adaptive histogram equalization. Traitement Du Signal, 39(2), 731–736.

Srinivasan, S., Raju, A.B.K., Mathivanan, S.K., Jayagopal, P., Babu, J.C., Sahu, A.K. 2023. Local-Ternary-pattern-based associated histogram equalization technique for cervical cancer detection. Diagnostics, 13(3), 548.

Sun, K. X., Cong, C. 2022. Research on chest abnormality detection based on improved YOLOv7 algorithm. In Proceedings - 2022 IEEE International Conference on Bioinformatics and Biomedicine, BIBM 2022, pp. 3884–3886.

Tang, F., Yang, F., Tian, X. 2023. Long-distance person detection based on YOLOv7. Electronics, 12(6), 1502.

Tian, J., Yuan, J., Liu, H. 2020. Road marking detection

based on MASK R-CNN instance segmentation model. In Proceedings - 2020 International Conference on Computer Vision, Image and Deep Learning (CVIDL), 246–249.

Wang, C.Y., Bochkovskiy, A., Liao, H.Y. M. 2023. YOLOv7: Trainable bag-of-freebies sets new state-of-the-art for real-time object detectors, 7464–7475.

Wu, D., Jiang, S., Zhao, E., Liu, Y., Zhu, H., Wang, W., Wang, R. 2022. Detection of Camellia oleifera fruit in complex scenes by using YOLOv7 and data augmentation. Applied Sciences, 12(22), 11318.

Zamani, A.S., Anand, L., Rane, K.P., Prabhu, P., Buttar, A.M., Pallathadka, H., Raghuvanshi, A., Dugbakie, B.N. 2022. Performance of machine learning and image processing in plant leaf disease detection. Journal of Food Quality, 2022, 1598796.